Supporting Information for:

Polarity and Air-Stability Transitions in Field-Effect Transistors Based on Fullerenes with Different Solubilizing Groups

Hojeong Yu,[a,†] *Han-Hee Cho,*[b,†] *Chul-Hee Cho,*[b] *Ki-Hyun Kim,*[b] *Dong Yeong Kim,*[a]

Bumjoon J. Kim,[b,*] *and Joon Hak Oh*[a,*]

[a]*School of Nano-Bioscience & Chemical Engineering, KIER-UNIST Advanced Center for Energy, Low Dimensional Carbon Materials Center, Ulsan National Institute of Science and Technology (UNIST), Ulsan 689-798, Korea*

[b]*Department of Chemical and Biomolecular Engineering, Korea Advanced Institute of Science and Technology (KAIST), Daejeon 305-701, Korea*

[*]Electronic mail: joonhoh@unist.ac.kr, bumjoonkim@kaist.ac.kr

[†]These authors contributed equally to this work.

Table of contents

Supplementary Figures S1-9

Supplementary Table S1-4

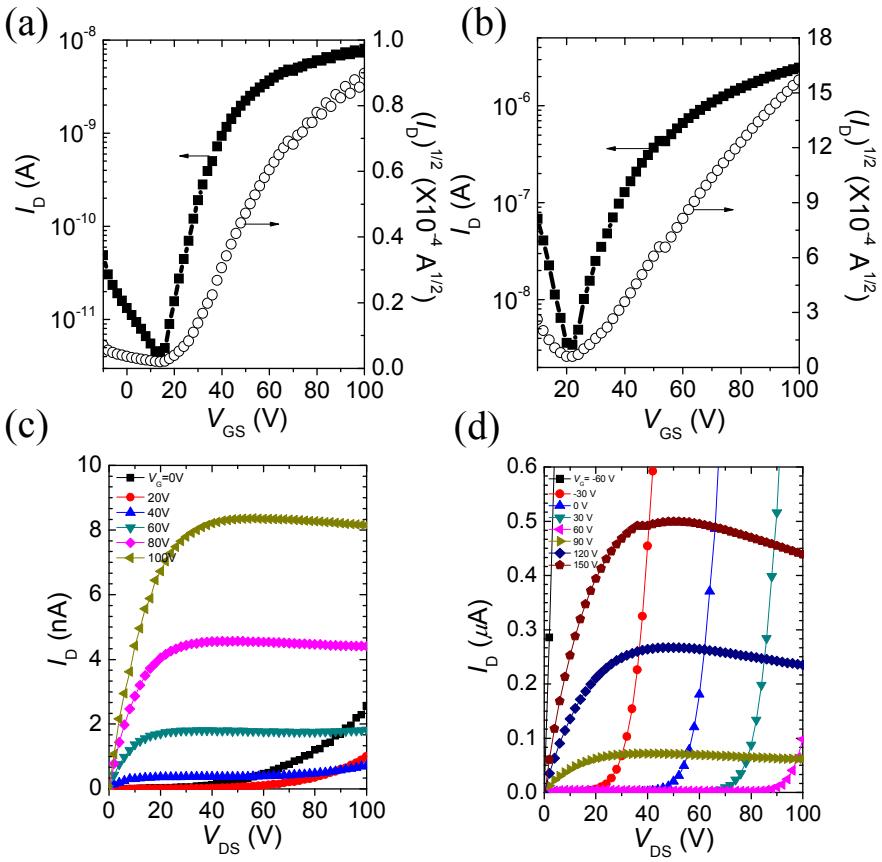

Figure S1. OFET performance of the fullerene bisadducts devices. Transfer characteristic of (a) OXCBA and (b) ICBA recorded at electron-enhancement mode (V_{DS}= +100 V). Output curves of (c) OXCBA and (d) ICBA recorded with increasing V_{GS} in steps of 20 V and 30 V, respectively, at electron-enhancement mode (The W/L values of OXCBA and ICBA films were 9.56 and 20, respectively).

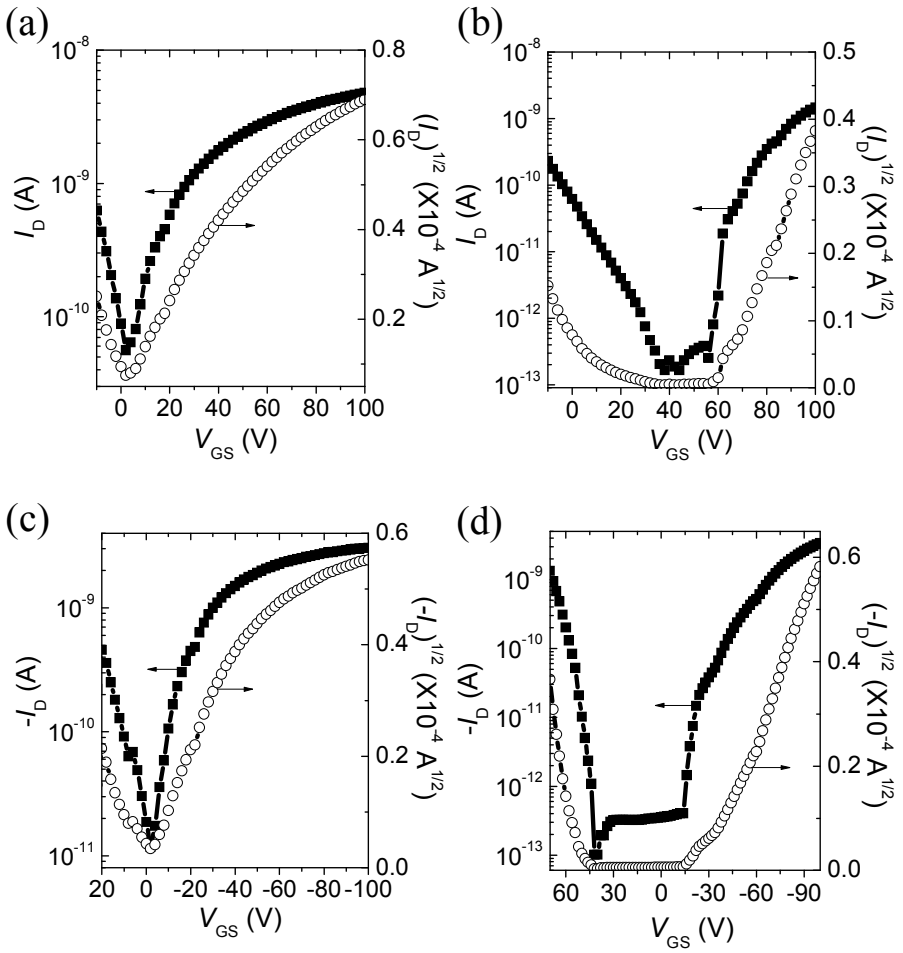

Figure S2. OFET performance of the fullerene trisadducts devices. Transfer characteristics of (a) OXCTA and (b) ICTA recorded at an electron-enhancement mode (V_{DS}= +100 V). Transfer characteristics of (c) OXCTA and (d) ICTA at a hole-enhancement mode (V_{DS}= -100 V). The *W*/*L* values of OXCTA and ICTA films were 11.79 and 20, respectively.

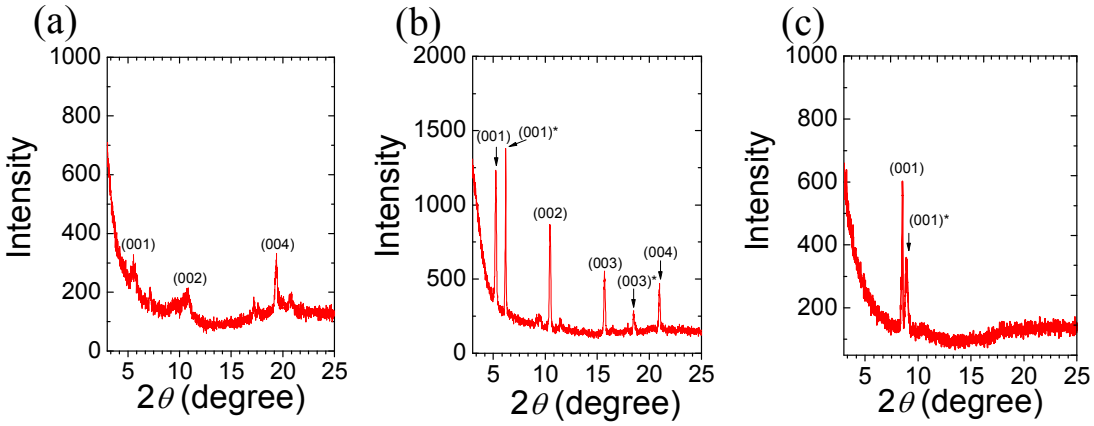

Figure S3. XRD patterns of drop cast (a) PCBM, (b) OXCMA, and (c) ICMA films on OTS-treated SiO_2/Si substrates. The diffraction peaks were observed under the same film thicknesses of approximately 1.5 μm. (* denotes the second polymorphic crystalline phase)

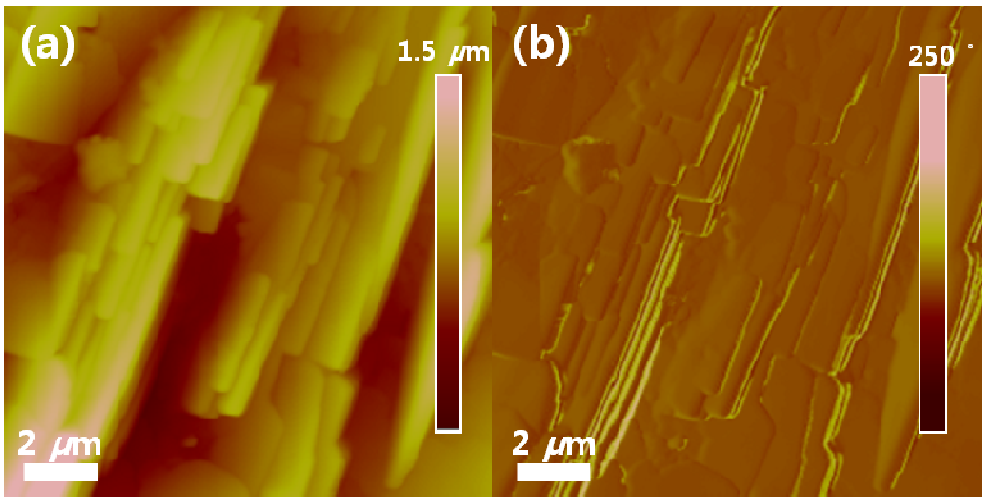

Figure S4. AFM topographic (a) height and (b) phase images of drop cast OXCMA film on OTS-treated SiO_2/Si substrates.

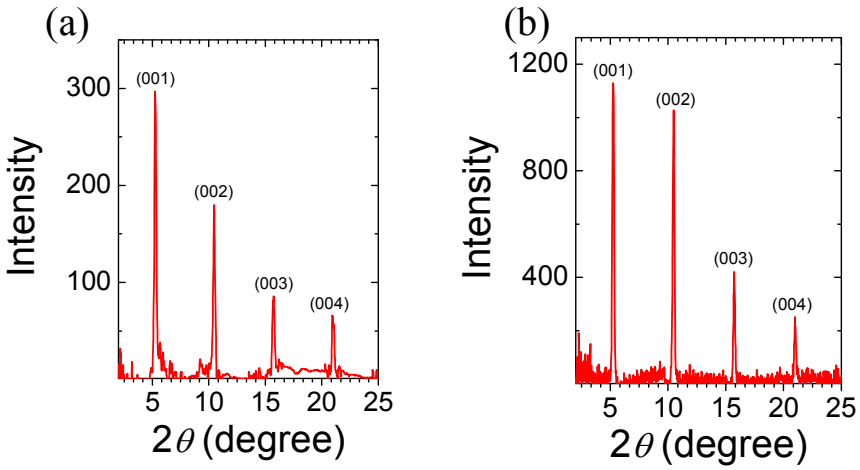

Figure S5. XRD patterns of solution sheared OXCMA films at a shearing rate of (a) 0.12 mm s^{-1} and (b) at 0.2 mm s^{-1} on OTS-treated SiO_2/Si substrates. The diffraction peaks were observed at the almost same 2θ ranges with different peak intensities under the same film thicknesses of approximately 1.5 μm.

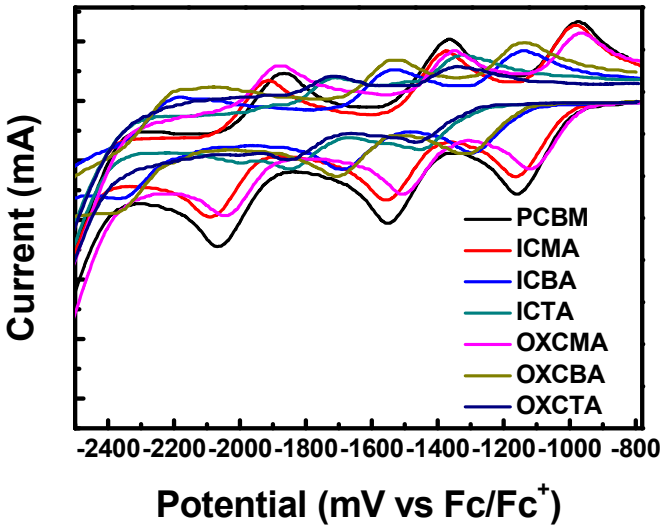

Figure S6. CV curves of the indene and *o*-xylene C_{60} multiadducts and PCBM with an Ag quasi-reference electrode

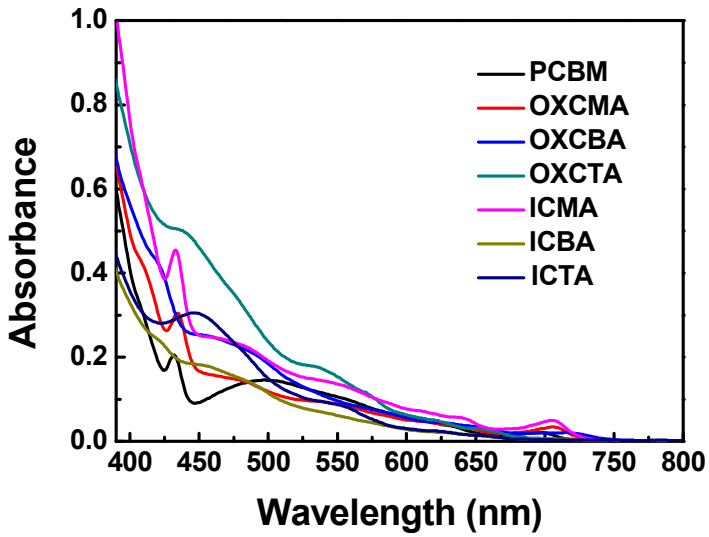

Figure S7. UV–vis absorption spectra of the indene and *o*-xylene C_{60} multiadducts and PCBM

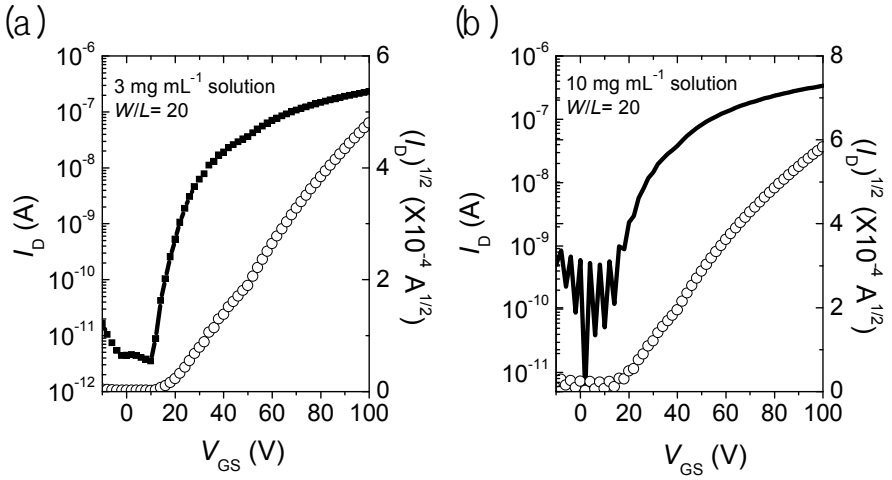

Figure S8. Effects of solution concentration on the mobility enhancement of OXCMA OFETs. Transfer characteristics were recorded from OXCMA OFETs prepared with a concentration of (a) 3 mg mL^{-1} and (b) 10 mg mL^{-1}, respectively. Mobility enhancement in the device fabricated from the higher concentration solution (W/L= 20, μ_e= 7.07 × 10^{-4} $cm^2V^{-1}s^{-1}$) was found to be a factor of 2.2 compared with the device fabricated using the lower concentration solution (W/L= 20, μ_e= 3.74 × 10^{-4} $cm^2V^{-1}s^{-1}$).

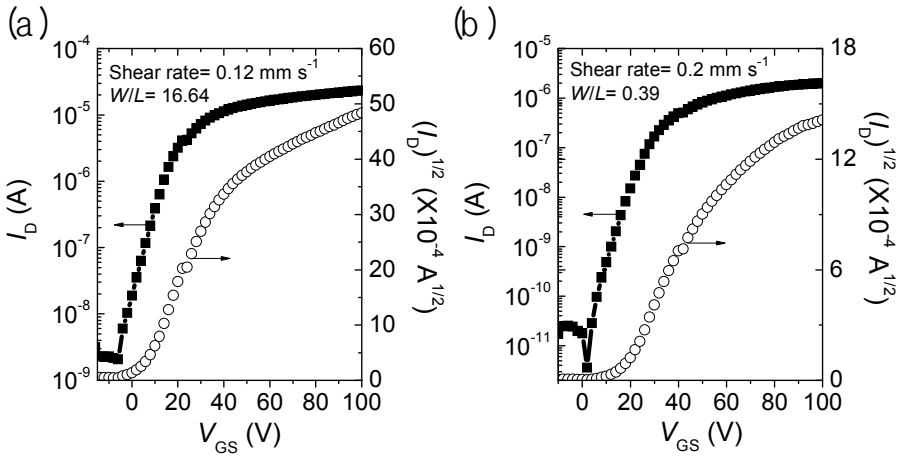

Figure S9. Effects of shearing rate on the mobility enhancement of OXCMA OFETs under identical solution concentrations of 10 mg mL^{-1} without doping. The representative transfer characteristics were obtained from OXCMA OFETs prepared under a shearing rate of (a) 0.12 mm s^{-1} and (b) 0.2 mm s^{-1}, respectively. Mobility enhancement in the device fabricated under the higher shearing rate (W/L = 0.39, μ_e = 0.549 $cm^2V^{-1}s^{-1}$) was found to be a factor of 2.2 compared with the device fabricated under the lower shearing rate (W/L = 16.64, μ_e= 0.191 $cm^2V^{-1}s^{-1}$).

Table S1. Summary of the HOMO and LUMO levels of PCBM, ICMA, ICBA, ICTA, OXCMA, OXCBA, and OXCTA.

	LUMO (eV) [a]	λ_{onset} (nm)[b]	E_g (eV) [c]	HOMO (eV)
PCBM	-3.85	728	1.70	-5.55
ICMA	-3.88	731	1.70	-5.58
ICBA	-3.67	740	1.68	-5.35
ICTA	-3.50	689	1.80	-5.30
OXCMA	-3.85	729	1.70	-5.55
OXCBA	-3.66	747	1.66	-5.32
OXCTA	-3.50	690	1.80	-5.30

[a]LUMOs measured by cyclic voltametry; [b]the long wavelength absorption edge on the UV-vis absorption spectra; [c]Optical bandgaps measured by the absorption onset of the UV-vis absorption spectra

Table S2. Electrical Performance of OFET Devices Based on the Drop Cast Thin Films of Fullerene Derivatives (These mobilities were measured in a N_2-filled glove-box)

Compound	*n*-type				*p*-type			
	$\mu_{e,max}$ [$cm^2V^{-1}s^{-1}$][a]	$\mu_{e,avg}$ [$cm^2V^{-1}s^{-1}$][b]	I_{on}/I_{off}	V_T [V]	$\mu_{h,max}$ [$cm^2V^{-1}s^{-1}$] [a]	$\mu_{h,avg}$ [$cm^2V^{-1}s^{-1}$]	I_{on}/I_{off}	V_T [V]
PCBM	0.0331	0.0206	2.5×10^5	16.3	N/A[c]	N/A[c]	N/A[c]	N/A[c]
OXCMA	0.0405	0.0274	1.6×10^3	8.6	N/A[c]	N/A[c]	N/A[c]	N/A[c]
OXCBA	7.36×10^{-5}	3.95×10^{-5}	3.1×10^3	33.7	6.17×10^{-6}	4.46×10^{-6}	7.5×10^4	-40.2
OXCTA	1.26×10^{-6}	7.73×10^{-7}	7.5×10^4	40.3	3.21×10^{-7}	2.54×10^{-7}	5.0×10^3	-3.8
ICMA	0.0507	0.0417	7.1×10^4	11.7	N/A[c]	N/A[c]	N/A[c]	N/A[c]
ICBA	4.63×10^{-3}	3.84×10^{-3}	7.5×10^4	32.8	5.97×10^{-4}	1.91×10^{-4}	2.2×10^2	-61.8
ICTA	2.90×10^{-6}	2.18×10^{-6}	3.2×10^3	53.2	1.05×10^{-5}	7.28×10^{-6}	1.3×10^6	-23.0

[a] The maximum mobility of the OFET devices
[b] The average mobility of the OFET devices
[c] The *p*-type performance of PCBM and fullerene monoadducts was not observed

Table S3. Peak Assignments for the Out-of-Plane XRD Patterns Obtained from Drop Cast PCBM, OXCMA, and ICMA Thin Films.

(00*n*)	**PCBM**		**OXCMA**		**ICMA**	
	2θ (degree)	*d*(*001*)-spacing (Å)	2θ (degree)	*d*(*001*)-spacing (Å)	2θ (degree)	*d(001)*-spacing (Å)
(001)	5.54	15.93	5.23 (6.19)[a]	16.86 (14.26)[a]	8.52 (8.88)[a]	10.37 (9.95)[a]
(002)	10.83	-	10.46	-	-	-
(003)	-	-	15.69	-	-	-
(004)	19.37	-	20.99	-	-	-

[a] polymorphic peak

Table S4. Peak Assignments for the Out-of-Plane XRD Patterns Obtained from OXCMA Thin Films Depending on the Solution Shearing Rate.

Coating method	(00*n*)	**OXCMA**	
		2θ (degree)	*d(001)*-spacing (Å)
Solution shearing at 0.12 mm s^{-1}	(001)	5.25	16.83
	(002)	10.47	-
	(003)	15.75	-
	(004)	20.93	-
Solution shearing at 0.2 mm s^{-1}	(001)	5.25	16.83
	(002)	10.47	-
	(003)	15.73	-
	(004)	21.01	-